Stochastic Hard-Sphere Dynamics for Hydrodynamics of Non-Ideal Fluids

Aleksandar Donev,[1] Berni J. Alder,[1] and Alejandro L. Garcia[2]

[1]*Lawrence Livermore National Laboratory, P.O.Box 808, Livermore, CA 94551-9900*
[2]*Department of Physics, San Jose State University, San Jose, California, 95192*

A novel stochastic fluid model is proposed with non-ideal structure factor consistent with compressibility, and adjustable transport coefficients. This Stochastic Hard Sphere Dynamics (SHSD) algorithm is a modification of the Direct Simulation Monte Carlo (DSMC) algorithm and has several computational advantages over event-driven hard-sphere molecular dynamics. Surprisingly, SHSD results in an equation of state and pair correlation function identical to that of a deterministic Hamiltonian system of penetrable spheres interacting with linear core pair potentials. The fluctuating hydrodynamic behavior of the SHSD fluid is verified for the Brownian motion of a nano-particle suspended in a compressible solvent.

With the increased interest in nano- and micro-fluidics, it has become necessary to develop tools for hydrodynamic calculations at the atomistic scale [1, 2]. Of particular interest is the modeling of flexible polymers in a flowing solvent for both biological (e.g., cell membranes) and engineering (e.g., micro-channel DNA arrays) applications. Typically the polymer chains are modeled using Molecular Dynamics (MD). For many applications, a realistic representation of the solvent and bidirectional coupling between the flow and the polymer motion is needed, for example, in the modeling of turbulent drag reduction. Previously, we introduced the Stochastic Event-Driven MD (SEDMD) algorithm that uses Direct Simulation Monte Carlo (DSMC) for the solvent coupled to deterministic EDMD for the polymer chain [3]. However, DSMC is limited to perfect gases. Efforts have been undertaken to develop solvents that have a *non-ideal* EOS, and that also have greater computational efficiency than brute-force molecular dynamics. Examples include the Lattice-Boltzmann (LB) method [4], Dissipative Particle Dynamics (DPD) [5], and Multi-Particle Collision Dynamics (MPCD) [6], each of which has its own advantages and disadvantages [1]. The *Stochastic Hard Sphere Dynamics* (SHSD) algorithm described in this Letter is based on successive stochastic collisions of variable hard-sphere diameters and is thermodynamically consistent (i.e., the direct calculation of compressibility from density fluctuations agrees with the density derivative of pressure). SHSD modifies previous algorithms for solving the Enskog kinetic equation [7, 8] while maintaining good efficiency.

In the SHSD algorithm randomly chosen pairs of approaching particles that lie less than a given diameter of each other undergo collisions as if they were hard spheres of diameter equal to their actual separation. The SHSD fluid is shown to be non-ideal, with structure and equation of state equivalent to that of a fluid mixture where spheres effectively interact with a repulsive linear core pairwise potential. We theoretically demonstrate this correspondence at low densities. Remarkably, we numerically find that this effective interaction potential, similar to the quadratic core potential used in many DPD variants, is valid at all densities. Therefore, the SHSD fluid, as DPD, is *intrinsically* thermodynamically-consistent, while non-ideal MPCD is only *numerically* thermodynamically-consistent for tuned choices of the parameters [6, 9].

As an algorithm, SHSD is similar in nature to DPD and has a similar computational complexity. In DPD, momentum is also stochastically exchanged between particles closer than a given distance. The essential difference is that DPD has a continuous-time formulation (a system of stochastic ODEs), where as the SHSD dynamics is discontinuous in time. This is similar to the difference between MD for continuous potentials and discontinuous potentials. Just as DSMC is a stochastic alternative to hard-sphere MD for low-density gases, SHSD is a stochastic modification of hard-sphere MD for dense gases. On the other hand, DPD is a modification of MD for smooth potentials to allow for larger time-steps and a hydrodynamically-consistent thermostat.

The SHSD algorithm is not as efficient as DSMC at a comparable collision rate. However, when low compressibility is desired, SHSD is several times faster than EDMD for hard spheres, the fastest available deterministic alternative. Low compressibility, for example, is desirable so that flows are kept subsonic even for high Reynolds number flows. Furthermore, SHSD has several important advantages over EDMD, in addition to its simplicity: (1) SHSD has several controllable parameters that can be used to change the transport coefficients and compressibility, while EDMD only has density; (2) SHSD is time-driven rather than event-driven thus allowing for easy parallelization; (3) SHSD can be more easily coupled to continuum hydrodynamic solvers, just like ideal-gas DSMC [10]. Strongly-structured particle systems, such as fluids with strong interparticle repulsion (e.g., hard spheres), are more difficult to couple to hydrodynamic solvers [11] than ideal fluids, such as MPCD or DSMC, or weakly-structured fluids, such as DPD or SHSD fluids.

The standard DSMC [12] algorithm starts with a time step where particles are propagated advectively, $\mathbf{r}_i' = \mathbf{r}_i + \mathbf{v}_i\Delta t$, and sorted into a grid of cells. Then, a certain number $N_{coll} \sim \Gamma_{sc} N_c(N_c-1)\Delta t$ of *stochastic collisions* are executed between pairs of particles randomly chosen from the N_c particles inside the cell. The conservative stochastic collisions exchange momentum and energy between two particles i and j that is not correlated with the actual positions of the particles. Typically the probability of collision is made proportional to the magnitude of the relative velocity $v_r = |\mathbf{v}_{ij}|$ by using a conventional rejection proce-

dure. DSMC, unlike MD, is not microscopically isotropic and does not conserve angular momentum, leading to an anisotropic stress tensor. To avoid such grid artifacts, all collision partners within a collision diameter D must be considered even if they are in neighboring cells, with a suitable modification of the trial collision frequency to maintain the same collision rate as DSMC. This grid-free variant will be called Isotropic DSMC (I-DSMC). The cost is that is the computational efficiency is reduced by a factor of $2-3$ due to the need to perform neighbor searches. Note that a pairwise Anderson thermostat proposed within the context of MD/DPD in Ref. [13] essentially adds I-DSMC collisions to ordinary MD and has very similar computational behavior. As in I-DSMC, in SHSD we consider particles in neighboring cells as collision partners in order to ensure isotropy of the collisional (non-ideal) component of the pressure tensor.

Because the collisional momentum exchange $m\Delta\mathbf{v}_{ij}$ in I-DSMC is not correlated with the displacement $\Delta\mathbf{r}_{ij}$ between the colliding particles, the virial $\langle\Delta\mathbf{v}_{ij}\cdot\Delta\mathbf{r}_{ij}\rangle$ vanishes giving an ideal-gas pressure. In order to introduce a non-trivial equation of state it is necessary to either give an additional displacement to the particles that is parallel to $\Delta\mathbf{v}_{ij}$, or to bias the momentum exchange $\Delta\mathbf{v}_{ij}$ to be (statistically) aligned to $\Delta\mathbf{r}_{ij}$. The former approach has already been investigated in the Consistent Boltzmann Algorithm (CBA) [14]; however, CBA is not thermodynamically consistent since it modifies the compressibility without affecting the density fluctuations (i.e., the structure of the fluid is still that of a perfect gas). A fully consistent approach is to require that the particles collide as if they are elastic hard spheres of diameter equal to the distance between them at the time of the collision. Such collisions produce a positive virial only if the particles are approaching each other, $v_n = -\mathbf{v}_{ij}\cdot\hat{\mathbf{r}}_{ij} > 0$, therefore, we reject collisions among particles that are moving apart. Furthermore, as for hard spheres, it is necessary to collide pairs with probability that is *linear* in v_n, which requires a further increase of the rejection rate and thus decrease of the efficiency. Without rejection based on v_n or v_r, temperature fluctuations would not be consistently coupled to the local pressure p_c because p_c would be $\sim\sqrt{T_c}$ instead of $p_c\sim T_c$. This is because the EOS of a fluid with no internal energy is linear in temperature, which from the virial theorem $p_c\sim\langle\Delta\mathbf{v}_{ij}\cdot\Delta\mathbf{r}_{ij}\rangle_c\sim\Gamma_{sc}\sqrt{T_c}$ implies that the *local* collisional frequency Γ_{sc} must be proportional to the square root of the *local* temperature T_c, $\Gamma_{sc}\sim\sqrt{T_c}$, as for hard spheres. For DSMC the collisional rules can be manipulated arbitrarily to obtain the desired transport coefficients, however, for non-ideal fluids thermodynamic requirements eliminate some of the freedom. Note that one can in fact mix SHSD collisions with I-DSMC collisions, that either take into account or ignore the v_n requirement, to introduce more tunable parameters in SHSD.

For sufficiently small time steps, the SHSD fluid can be considered as a simple modification of the standard hard-sphere fluid. Particles move ballistically in-between collisions. When two particles i and j are less than a diameter apart, $r_{ij}\le D$, there is a probability rate $(3\chi/D)v_n\Theta(v_n)$ for them to collide as if they were elastic hard spheres with a variable diameter $D_S = r_{ij}$. Here Θ is the Heaviside function, and χ is a dimensionless parameter determining the collision frequency. The prefactor $3/D$ has been chosen so that for an ideal gas the average collisional rate would be χ times larger than that of a low-density hard-sphere gas with density (volume fraction) $\phi=\pi ND^3/(6V)$.

In order to understand properties of the SHSD fluid as a function of ϕ and χ, we consider the equilibrium pair correlation function g_2 at low densities, where correlations higher than pairwise can be ignored. We consider the cloud of point walkers ij representing the $N(N-1)/2$ pairs of particles, each at position $\mathbf{r}=\mathbf{r}_i-\mathbf{r}_j$ and with velocity $\mathbf{v}=\mathbf{v}_i-\mathbf{v}_j$. At equilibrium, the distribution of the point walkers in phase space will be $f(\mathbf{v},\mathbf{r}) = f(v_r,r)\sim g_2(r)\exp(-mv_n^2/4kT)$. Inside the core $r<D$ this distribution of pair walkers satisfies a kinetic equation

$$\frac{\partial f}{\partial t}+v_n\frac{\partial f}{\partial r}=v_n\Gamma_0 f,$$

where $\Gamma_0 = 3\chi/D$ is the collision frequency. At equilibrium, $\partial f/\partial t = 0$ and v_n cancels, consistent with choosing collision probability linear in $|v_n|$. Thus $dg_2/dx = 3\chi g_2\Theta(1-x)$, with solution $g_2(x) = \exp\left[3\chi(x-1)\right]$ for $x\le 1$ and $g_2(x) = 1$ for $x>1$, where $x = r/D$. Indeed, numerical experiments confirmed that at sufficiently low densities the equilibrium g_2 for the SHSD fluid has this exponential form inside the collision core. This low density result is equivalent to $g_2^U = \exp[-U(r)/kT]$, where $U(r)/kT = 3\chi(1-x)\Theta(1-x)$ is an effective *linear core* pair potential similar to the quadratic core potential used in DPD. Remarkably, it was found *numerically* that this repulsive potential can predict exactly $g_2(x)$ at *all* liquid densities. Figure 1 shows a comparison between the pair correlation function of the SHSD fluid on one hand, and a Monte Carlo calculation using the linear core pair potential on the other, at several densities. Also shown is a numerical solution to the hyper-netted chain (HNC) integral equations for the linear core system, inspired by its success for the Gaussian core model [15]. The excellent agreement at all densities permits the use of the HNC result in practical applications, notably the calculation of the transport coefficients.

Interestingly, in the limit $\chi\to\infty$ the SHSD algorithm reduces to hard-sphere (HS) molecular dynamics. In fact, if the density ϕ is smaller than the freezing point for the HS system, the structure of the SHSD fluid approaches, as χ increases, that of the HS fluid. For higher densities, if χ is sufficiently high, crystallization is observed in SHSD, either to the usual hard-sphere crystals if ϕ is lower than the close-packing density, or if not, to an unusual partially ordered state with multiple occupancy per site, typical of weakly repulsive potentials.

An exact BBGKY-like hierarchy of Master equations for the s-particle distribution functions of the SHSD fluid is given in Ref. [16]. For the first equation of this BBGKY hierarchy, valid at low densities, we can neglect correlations

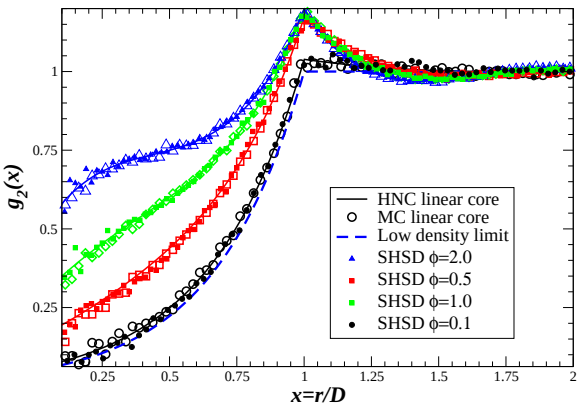

Figure 1: (Color online) Equilibrium pair correlation function of the SHSD fluid (solid symbols), compared to MC (open symbols) and HNC calculations (solid lines) for the linear core system, at various densities and $\chi = 1$.

other than pair ones and approximate $f_2(\mathbf{r}_1, \mathbf{v}_1, \mathbf{r}_2, \mathbf{v}_2) = g_2(\mathbf{r}_{12}) f_1(\mathbf{r}_1, \mathbf{v}_1) f(\mathbf{r}_2, \mathbf{v}_2)$. With this assumption we obtain a stochastic Enskog equation similar to a revised Enskog equation for hard spheres but with a smeared distribution of hard-sphere diameters, as studied in Ref. [17]. The Chapman-Enskog expansion carried out in Ref. [17] produces the equation of state (EOS) $p = PV/NkT$, and approximations to the self-diffusion coefficient ζ, the shear η and bulk η_B viscosities, and thermal conductivity κ of the SHSD fluid. The expressions ultimately give the transport coefficients in terms of various integer moments of $g_2(x)$, $x_k = \int_0^1 x^k g_2(x) dx$, specifically, $p - 1 = 12\phi\chi x_3$, $\zeta/\zeta_0 = \sqrt{\pi}/(48\phi\chi x_2)$, $\eta_B/\eta_0 = 48\phi^2\chi x_4/\pi^{3/2}$, and

$$\eta/\eta_0 \text{ or } \kappa/\kappa_0 = \frac{c_1}{\sqrt{\pi}\chi x_2}(1 + c_2\phi\chi x_3)^2 + c_3\eta_B/\eta_0,$$

where $\zeta_0 = D\sqrt{kT/m}$, $\eta_0 = D^{-2}\sqrt{mkT}$ and $\kappa_0 = kD^{-2}\sqrt{kT/m}$ are natural units, and $c_1 = 5/48$, $c_2 = 24/5$ and $c_3 = 3/5$ for η, while $c_1 = 25/64$, $c_2 = 24/5$ and $c_3 = 3/5$ for κ.

The above formula for the pressure is exact and is equivalent to the virial theorem for the linear core potential, and thus thermodynamic consistency between $g_2(x)$ and $p(\phi)$ is guaranteed. In the inset in the top part of Fig. 2, we directly demonstrate the thermodynamic consistency of SHSD by comparing the compressibility calculated from the EOS, $S_c = (p + \phi dp/d\phi)^{-1}$, to the structure factor at the origin $S_0 = S(\omega = 0, k = 0)$. Furthermore, good agreement is found between the adiabatic speed of sound $c_s^2 = S_0^{-1} + 2p^2/3$ and the location of the Brillouin lines in the dynamic structure factor $S(\omega; k)$ for small k values. In Fig. 2, we also compare the theoretical predictions for η utilizing the HNC approximation for g_2 to the ones directly calculated from SHSD. Surprisingly, good agreement is found for the shear viscosity at all densities. The corresponding results for ζ show significant ($\sim 25\%$) deviations for the self-diffusion coefficient at higher densities because of corrections due to higher-order correlations.

As an illustration of the correct hydrodynamic behavior of the SHSD fluid and the significance of compressibility, we study the velocity autocorrelation function (VACF)

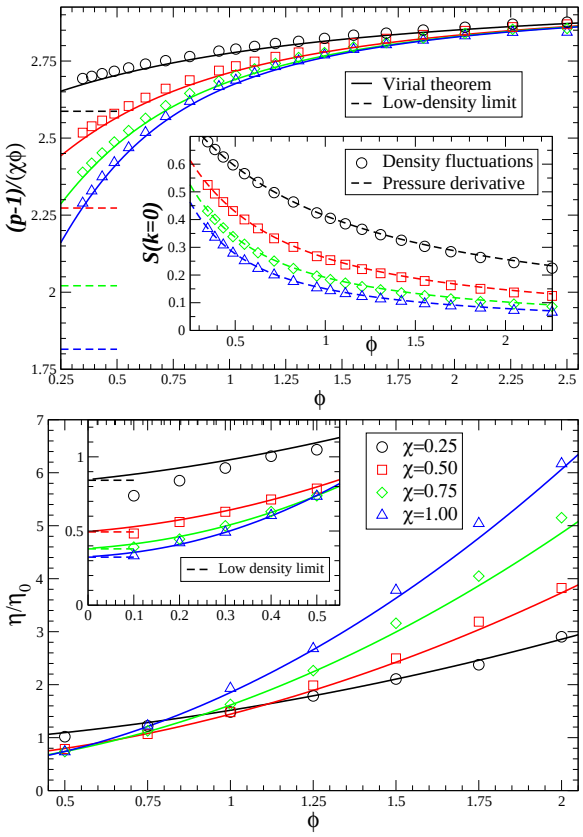

Figure 2: (Color online) Comparison between numerical results for SHSD at several collision frequencies (different symbols) with predictions based on the stochastic Enskog equation using the HNC $g_2(x)$ (solid lines). The low-density approximations are also indicated (dashed lines). (*Top*) Normalized equation of state. The inset compares the compressibility (pressure derivative, dashed lines) to the structure factor at the origin $S(k \to 0)$ (symbols), measured using a direct Fourier transform of the particle positions for small k and extrapolating to $k = 0$. (*Bottom*) The shear viscosity at high and low densities (inset), as measured using an externally-forced Poiseuille flow. There are significant corrections (Knudsen regime) for large mean free paths (i.e., at low densities and low collision rates).

$C(t) = \langle v_x(0) v_x(t) \rangle$ for a single neutrally-buoyant hard sphere of mass m and radius R suspended in an SHSD fluid of mass density ρ. This problem is relevant to the modeling of polymer chains or (nano)colloids in solution, and led to the discovery of a long power-law tail in $C(t)$ [18, 19]. Here the solvent-solvent particles interact as in SHSD. The solvent-solute interaction is treated as if the SHSD particles are hard spheres of diameter D_s, chosen to be somewhat smaller than their interaction diameter with other solvent particles (specifically, we use $D_s = D/4$) for computational efficiency reasons, using an event-driven algorithm [3]. Upon collision the relative velocity of the solvent particle is reversed in order to provide a no-slip condition at the surface of the suspended sphere [3, 18] (slip boundaries give qualitatively identical results). For comparison, an ideal solvent of comparable viscosity is also simulated.

Theoretically, $C(t)$ has been calculated from the linearized (compressible) fluctuating Navier-Stokes (NS) equations [18]. The results are analytically complex even in the Laplace domain, however, at short times an invis-

cid compressible approximation applies. At large times the compressibility does not play a role and the incompressible NS equations can be used to predict the long-time tail. At short times, $t < t_c = 2R/c_s$, the major effect of compressibility is that sound waves generated by the motion of the suspended particle carry away a fraction of the momentum, so that the VACF quickly decays from its initial value $C(0) = kT/m$ to $C(t_c) \approx kT/M$, where $M = m + 2\pi R^3\rho/3$. At long times, $t > t_{visc} = 4\rho R_H^2/3\eta$, the VACF decays as in an incompressible fluid, with an asymptotic power-law tail $(kT/m)(8\sqrt{3\pi})^{-1}(t/t_{visc})^{-3/2}$, in disagreement with predictions based on the Langevin equation (Brownian dynamics), $C(t) = (kT/m)\exp(-6\pi R_H\eta t/m)$. We have estimated the effective (hydrodynamic) colloid radius R_H from numerical measurements of the Stokes friction force $F = -6\pi R_H\eta v$.

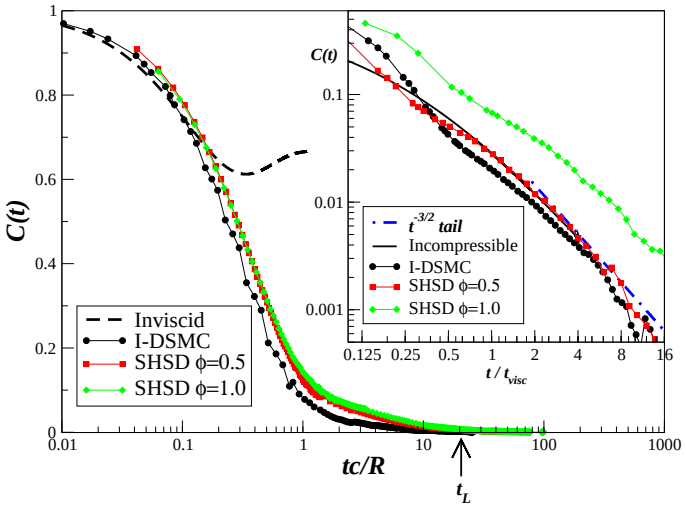

Figure 3: (Color online) The velocity autocorrelation function for a neutrally buoyant hard sphere suspended in a non-ideal SHSD ($\chi = 1$) solvent at two densities (symbols), as well as an ideal I-DSMC solvent ($\phi = 0.5$, $\chi = 0.62$, symbols), at short and long times (inset). For the more compressible (less viscous) fluids the long time tails are statistically measurable only up to $t/t_{visc} \approx 5$. The theoretical predictions based on the inviscid, for short times, or incompressible, for long times, Navier-Stokes equations are also shown (lines). The diameter of the nano-colloidal particle is only $2.5D$, although we have performed simulations using larger spheres as well with very similar results. Since periodic boundary conditions were used we only show the tail up to about the time at which sound waves generated by its periodic images reach the particle, $t_L = L/c_s$.

In Fig. 3 numerical results for the VACF for an I-DSMC solvent and an SHSD solvent at two different densities are compared to the theoretical predictions. It is seen, as predicted, that the compressibility or the sound speed c_s, determines the early decay of the VACF. The exponent of the power-law decay at large times is also in agreement with the hydrodynamic predictions. The coefficient of the VACF tail agrees reasonably well with the hydrodynamic prediction for the less dense solvents, however, there is a significant deviation of the coefficient for the densest solvent, perhaps due to ordering of the fluid around the suspended sphere, not accounted for in continuum theory.

In closing, we should point out that for reasonable values of the collision frequency ($\chi \sim 1$) and density ($\phi \sim 1$) the SHSD fluid is still relatively compressible compared to a dense liquid, $c_s^2 < 10$. Indicative of this is that the diffusion coefficient is large relative to the viscosity as in typical DPD simulations, so that the Schmidt number $S_c = \eta(\rho\zeta)^{-1}$ is less than 10 instead of being on the order of 100-1000. Achieving higher c_s or S_c requires high collision rates (for example, $\chi \sim 10^4$ is used in Ref. [13]) and appropriately smaller time steps to ensure that there is at most one collision per particle per time step, and thus a similar computational effort as in molecular dynamics. The advantage of SHSD is its simplicity, easy parallelization, and simpler coupling to continuum methods such as fluctuating hydrodynamics [10].

This work performed under the auspices of the U.S. Department of Energy by Lawrence Livermore National Laboratory under Contract DE-AC52-07NA27344 (LLNL-JRNL-401745). We thank Salvatore Torquato, Frank Stillinger, Ard Louis, Andres Santos, and Jacek Polewczak for their assistance and advice.

[1] H. Noguchi, N. Kikuchi, and G. Gompper, Europhysics Letters **78**, 10005 (2007).
[2] G. D. Fabritiis, M. Serrano, R. Delgado-Buscalioni, and P. V. Coveney, Phys. Rev. E **75**, 026307 (2007).
[3] A. Donev, A. L. Garcia, and B. J. Alder, J. Comp. Phys. **227**, 2644 (2008).
[4] L.-S. Luo, Phys. Rev. E **62**, 4982 (2000).
[5] I. Pagonabarraga and D. Frenkel, Molecular Simulation **25**, 167 (2000).
[6] T. Ihle, E. Tüzel, and D. M. Kroll, Europhys. Lett. **73**, 664 (2006).
[7] A. Frezzotti, Phys. Fluids **9**, 1329 (1997).
[8] J. M. Montanero and A. Santos, Phys. Fluids **9**, 2057 (1997).
[9] E. Tüzel, T. Ihle, and D. M. Kroll, Math. and Comput. in Simul. **72**, 232 (2006).
[10] S. A. Williams, J. B. Bell, and A. L. Garcia, SIAM Multiscale Modeling and Simulation **6**, 1256 (2008).
[11] R. Delgado-Buscalioni and G. D. Fabritiis, Phys. Rev. E **76**, 036709 (2007).
[12] F. J. Alexander and A. L. Garcia, Computers in Physics **11**, 588 (1997).
[13] C. P. Lowe, Europhysics Letters **47**, 145 (1999).
[14] F. J. Alexander, A. L. Garcia, and B. J. Alder, Phys. Rev. Lett. **74**, 5212 (1995).
[15] A. A. Louis, P. G. Bolhuis, and J. P. Hansen, Phys. Rev. E **62**, 7961 (2000).
[16] M. Lachowicz and M. Pulvirenti, Archive for Rational Mechanics and Analysis **109**, 81 (1990).
[17] J. Polewczak and G. Stell, J. Stat. Phys. **109**, 569 (2002).
[18] J. T. Padding and A. A. Louis, Phys. Rev. E **74**, 031402 (2006).
[19] M. W. Heemels, M. H. J. Hagen, and C. P. Lowe, J. Comp. Phys. **164**, 48 (2000).